

From Gas to Stars Over Cosmic Time

Mordecai-Mark Mac Low^{1,2*}

¹Department of Astrophysics, American Museum of Natural History
79th Street at Central Park West, New York, NY 10024, USA

²Zentrum der Astrophysik der Universität Heidelberg, Institut für Theoretische Astrophysik
Albert-Ueberle-Str. 2, 69121 Heidelberg, Germany

*To whom correspondence should be addressed; E-mail: mordecai@amnh.org.

From the time the first stars formed over 13 billion years ago to the present, star formation has had an unexpectedly dynamic history. At first, the star formation rate density increased dramatically, reaching a peak 10 billion years ago more than ten times the present day value. Observations of the initial rise in star formation remain difficult, poorly constraining it. Theoretical modeling has trouble predicting this history because of the difficulty in following the feedback of energy from stellar radiation and supernova explosions into the gas from which further stars form. Observations from the ground and space with the next generation of instruments should reveal the full history of star formation in the universe, while simulations appear poised to accurately predict the observed history.

Once, there were no stars. This simple, yet profound, statement is an inevitable consequence of Big Bang cosmology. Observations of the cosmic microwave background reveal that at the time of its emission some 300,000 years after the Big Bang, the Universe was filled with hydrogen and helium having a density uniform to a few parts in 10^5 (1, 2). Understanding how that gas evolved into the Universe filled with stars that we observe today, 13.798 ± 0.037 billion years later (3, 4), remains one of the most important goals of modern astrophysics.

The ordinary matter from which stars form makes up only $4.63 \pm 0.0024\%$ of the total mass-energy of the Universe and 17% of the matter (5), with the rest being made up of not yet identified cold dark matter, and dark energy. Star formation traces the gravitational collapse of the dark matter into the cosmic web in a universe whose expansion is currently dominated by dark energy.

Star formation Stars form when gravity causes interstellar gas and dust—the interstellar medium—to collapse towards regions of higher density, while radiative cooling prevents the temperature from increasing as densities get higher, so that pressure cannot prevent collapse. Collapse ultimately continues until central temperatures and pressures rise high enough for nuclear fusion to begin, heating the gas sufficiently to counterbalance the force of gravity and maintain hydrostatic equilibrium. This process occurs over a time of order the free-fall time of the gas $t_{\text{ff}} \sim (G\rho)^{-1/2}$, depending only on ρ , the mass density of the gas, where G is the gravitational constant. The mass of a region capable of gravitational collapse is given by the Jeans (*120*) mass

$$M_J = (\pi/6)G^{-3/2}\rho^{-1/2}c_s^3,$$

where c_s is the sound speed of the gas, which depends on the the temperature as $T^{1/2}$.

The collapse of dark matter from small perturbations into the gravitationally bound structures first identified as halos around galaxies can be followed by the Press-Schechter (6, 7) analytic excursion-set formalism. However, the properties of the stellar populations that form within those halos, in visible galaxies, depend critically on nonlinear physics including magnetized gas dynamics, radiative transfer, and nuclear fusion. We are ultimately forced to rely on numerical simulations of galaxy formation incorporating approximate treatments of these processes in order to predict the observable outcomes of cosmological theory.

The approximations used in these models rely on a detailed understanding of the smaller-scale physics determining star formation. Feedback of energy into the interstellar and intergalactic gas from ionizing ultraviolet (UV) radiation and supernova explosions from stars, and from high-velocity outflows and radiation from supermassive black holes, has been extremely difficult to model well enough to predict the star formation history of galaxies. Models that neglect feedback or understate its importance predict far too much star formation at early times (8, 9). Because of its central importance to modern models of star formation, I explore this topic in some detail in this review.

Star Formation History of the Universe

Star formation in the Universe can be described using the star formation rate (SFR) density at any time, often expressed in units of solar masses per cubic megaparsec per year. After a slow start, the SFR density in the observed Universe peaked some 10 billion years ago, when stars formed an order of magnitude faster than they do in the present epoch (*10–12*). Light emitted then has been redshifted by the expansion of the Universe to longer wavelengths by a factor of $(1+z) = 3$, so we refer to that era¹ as being at redshift $z = 2$. The time dependence of the SFR at higher redshifts (greater lookback times) remains uncertain, leaving the time of formation of

¹The exact relationship between redshift and lookback time is nonlinear and depends on the actual expansion law of the Universe.

the first stars poorly constrained (12–14). Two major lines of evidence, from imaging galaxies, and gamma ray bursts, give apparently conflicting results (14–16), that in turn must agree with two constraints: the range of time over which the intergalactic medium was reionized by UV radiation from stars, and the well-observed density of stars at $z = 4$.

The first line of evidence relies on the detection of high redshift galaxies by photometry in multiple colors. Even broad band photometry can detect the sharp cutoff in galactic emission in the far UV beyond the 91.2 nm Lyman limit, the wavelength of light that can ionize hydrogen, the most abundant element, and thus will be absorbed by it. Galaxies at high redshifts have this Lyman break redshifted into visible or even infrared light, where it can be observed from large, ground-based telescopes. A galaxy that is bright in colors with wavelengths longer than the redshifted break, but disappears below it, can be identified as being at a specific redshift (17). Lyman break galaxies observed out to $z > 8$ (6×10^8 yr after the Big Bang) can be used to determine the SFR density as a function of redshift [e.g. (18)]. However, the faintest galaxies at each redshift cannot be detected, so their contribution must be extrapolated from the distribution of the brighter observed galaxies. Only taking into account the directly observed galaxies leads to the conclusion that the star formation rate drops off rather quickly at high redshift (14, 15, 19) as shown by the blue points in Fig. 1. However, this is in tension with the first constraint, because it would imply a reionization redshift somewhat later than the current concordance value $z = 10.1 \pm 1.0$ (5).

Gamma-ray bursts provide the second line of evidence. These intense flashes of tightly beamed, gamma-ray light produced in occasional supernova explosions (20) are bright enough to be observed back to $z > 8$. Derivation of the SFR associated with the host galaxies of such high-redshift gamma-ray bursts depends on calibrations at lower redshifts, though. Extension of these calibrations to high redshift requires determination of how the incidence of gamma ray bursts as a function of the star formation rate evolves with redshift (14–16). One hypothesis is that gamma ray bursts occur primarily in galaxies with low abundances of heavy elements, which form a greater fraction of the population at high redshift. However, the star formation rate derived from that hypothesis (the red points in Fig. 1) violates the second constraint, predicting too high a stellar density by $z = 4$ (16). Similarly, the model shown by the green line in Figure 1, that includes this hypothesis, as well as a physically-motivated minimum mass of dark matter halo in which stars can form, still predicts slightly less star formation than suggested by the red points. This suggests that some other effect must also be acting (14, 16). The strength of this effect can be empirically derived by measuring the fraction of gamma ray burst host galaxies detectable at redshifts $z = 5$ and $z = 6$ (14).

Numerical Simulations

Numerical simulations a decade ago [e.g. (9)] predicted that the peak in star formation should occur at $z \sim 6$. The contradiction to the observations of the well-observed peak at $z \sim 2$ occurs in large part because neglecting feedback, or including it by standard recipes (21), leads

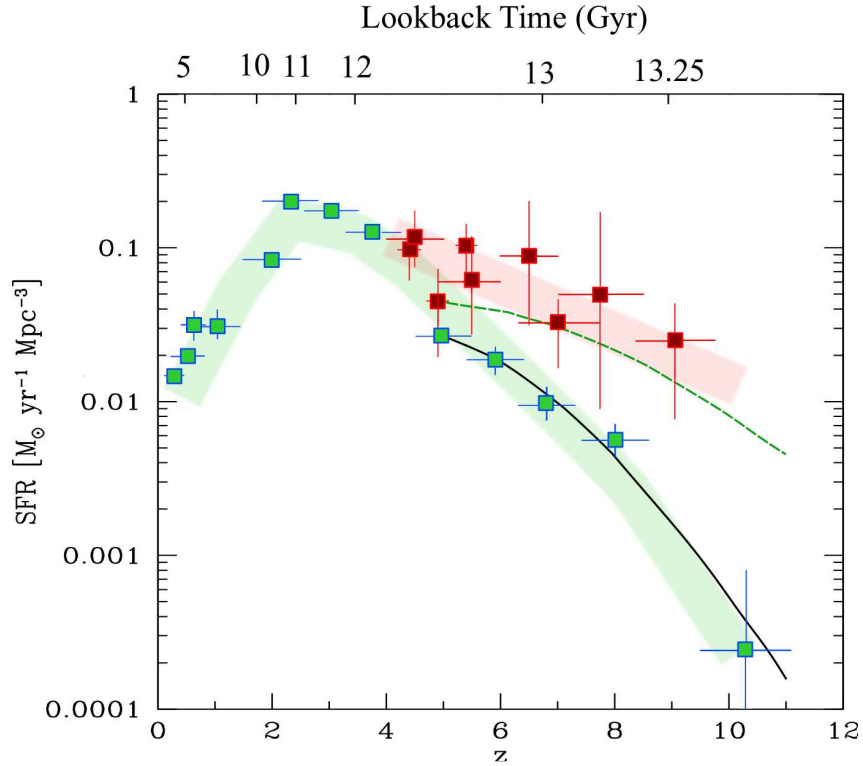


Figure 1: **Cosmic history of star formation.** The cosmic history of star formation in the universe versus redshift z or lookback time (14). Star formation peaked some 10 billion years ago at a rate ten times as high as the modern era. At high redshift, the lower estimates outlined in green rely on observations of high-redshift Lyman break galaxies, neglecting those below the detection limit (18), whereas the upper estimates outlined in red depend on the star formation intensity per gamma-ray burst (15). The lines show model predictions (16, 127), integrated over either the range of galaxies included in the Lyman break galaxy survey (black solid), or down to the expected lower limit for the mass of star forming galaxies (green dashed).

to overproduction of stars at early times. The alternative to date has been reliance on ad hoc models of strong feedback, both from stars and supermassive black holes, to suppress that early star formation, in order to agree with the observations.

This is because simulations capturing cosmological scales have been unable to model the interstellar medium within galaxies with sufficient resolution to follow the energetics of stellar feedback successfully. This leads to the classical overcooling problem. Without local feedback that transfers realistic amounts of energy to the interstellar medium, the SFR can be an order of magnitude higher than observed, even in models of modern galaxies (9, 22–28).

Another reason for requiring ad hoc models of energetic feedback, which I will not focus on here, is that accretion into clusters of galaxies produces huge reservoirs of hot gas. The accretion of this low density, hot gas onto massive elliptical galaxies must be throttled. It is much easier to prevent accretion onto galaxies of low density gas that can not radiatively cool easily, than it is to reheat and expel already cooled and accreted gas. The required heating likely comes from the jets driven by supermassive black holes in active galactic nuclei, rather than stars.

Feedback models typically fail because of unphysical cooling in poorly resolved regions of hot gas. Interstellar and intergalactic gas cools radiatively (29, 30): inelastic collisions excite electrons into higher energy levels, while slowing down the colliding particles (effectively reducing the temperature of the gas). The excited electrons then drop back to the ground state releasing photons. So long as the densities are low enough for collisions not to deexcite the electrons prior to radiation, and the opacity of the gas and dust is low enough to allow escape of the photons from the system, these inelastic collisions lead to energy loss, and thus cooling. Interstellar and intergalactic gas away from the very densest cores of star forming regions typically satisfies both of these conditions.

Because radiative cooling relies on collisions, its strength $\dot{E} = -n^2\Lambda(T)$ depends on the square of the number density n , as well as having a strong temperature dependence $\Lambda(T)$ from the distribution of available energy levels for electron excitation. Crucially, the value of $\Lambda(T)$ for $T = 10^5$ K gas in ionization equilibrium exceeds by more than an order of magnitude that for hot 10^6 K or cool 10^4 K gas [Fig. 2a, (30)]. The elevated cooling around 10^5 K occurs because of the ability of collisions in that temperature range to excite the strong resonance lines of lithium-like ions of carbon, oxygen, and nitrogen, the most common elements heavier than helium.

The temperature and density dependence of the cooling function leads to two serious problems for numerical simulations. First, supernova explosions drive blast waves that shock gas to temperatures above 10^6 K, so that it only cools with difficulty. However, if stellar feedback energy is fed into the grid of a numerical simulation too slowly, or over too large a volume, it will only raise the temperature into the 10^5 K range or lower, so that the energy will promptly radiate without exerting dynamical effects. Second, simulations of gas flow usually require several zones to resolve interfaces between gas with different properties, such as hot and rarefied or cold and dense. Within such an interface, the resolution of the numerical grid determines the amount of intermediate temperature gas, rather than the physics of the interface (See Fig. 2b). In poorly

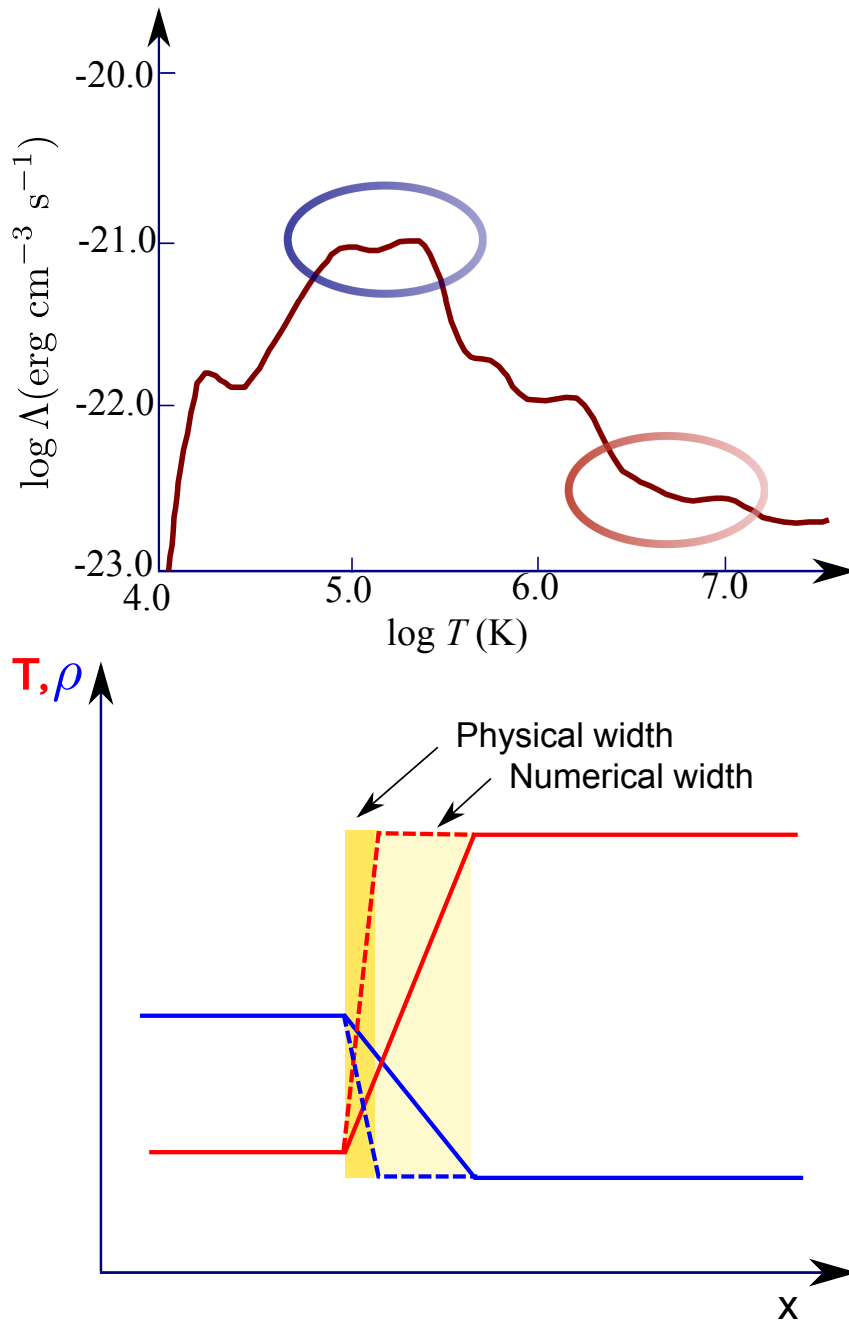


Figure 2: **Cooling of interstellar gas.** (a) The temperature dependence of the cooling function $\Lambda(T)$ from (30), showing the order of magnitude higher cooling rate at around 10^5 K (red circle) compared to 10^{6-7} K (blue circle). (b) Sketch of how unphysical cooling can occur at poorly resolved numerical interfaces when too much intermediate temperature gas is present.

resolved models, such interfaces capture large volumes of gas that cools unphysically. Over 25 years ago, Tomisaka (31) already demonstrated that the evolution of superbubbles formed by multiple supernova explosions from an association of OB stars could not be adequately simulated with 5 pc (16 light year) resolution because of such strong numerical overcooling (32). For models of the diffuse interstellar medium of the Milky Way galaxy ($0.01 < n < 100 \text{ cm}^{-3}$), it has been demonstrated that 2 pc (6.5 light year) grid cells resolve interfaces well enough to avoid dynamically important loss of energy from hot gas (33–35). Such a model, from (35) is shown in Movie S1.

How Does Stellar Feedback Inhibit Star Formation?

Energetic feedback from stars heats the interstellar gas through radiative ionization, and drives strong shock waves through it from supernova explosions, leaving it in a characteristic state of supersonic, highly compressible turbulence. This differs in its properties from the almost incompressible turbulence familiar from the terrestrial atmosphere and ocean because of the strong density fluctuations produced by the shock waves, and the strong vorticity sheets produced at shock intersections.

Such highly compressible turbulence both promotes and prevents gravitational collapse. We can heuristically estimate which effect wins by examining the dependence of the Jeans critical mass for gravitational collapse (eq. 1) $M_J \propto \rho^{-1/2} c_s^3$ on the root-mean-square turbulent velocity v_{rms} (36). In the classical picture, turbulence is treated as an additional pressure (37, 38), so that we can define an effective sound speed $c_{s,\text{eff}}^2 = c_s^2 + v_{\text{rms}}^2/3$. This additional effective pressure increases the Jeans mass by $M_J \propto v_{\text{rms}}^3$, inhibiting collapse. On the other hand, shock waves with Mach number $\mathcal{M} = v_s/c_s$ in an isothermal medium cause density enhancements with density ratio $\rho_s/\rho_0 = \mathcal{M}^2$. These turbulent compressions decrease the Jeans mass by $M_J \propto \rho_s^{-1/2}$, assuming that the shocks typically have shock velocity $v_s \simeq v_{\text{rms}}$.

When we combine the effects of increased pressure and increased density, we find that

$$M_J \propto \left(\frac{c_s}{v_{\text{rms}}} \right) \left(c_s^2 + \frac{v_{\text{rms}}^2}{3} \right)^{3/2} \propto v_{\text{rms}}^2 \quad (1)$$

for $v_{\text{rms}} \gg c_s$. Thus, highly supersonic turbulence strongly inhibits collapse. Because turbulence acts intermittently, however, it still promotes collapse locally, in shock compressed regions, even though its net effect is to inhibit collapse globally. Therefore, a region with mass lower than the Jeans mass globally because of turbulence can still have isolated regions of local collapse, as shown in isothermal simulations (39). The role of compression was isolated in simulations by (40) who increased the average density with the dependence on the Mach number required to balance the turbulent support term. Even higher resolution simulations using adaptive mesh refinement (41) show that the star formation efficiency can be expressed in terms of the ratio of the crossing time $t_x = L/2v_{\text{rms}}$ for a region of size L to the free-fall time t_{ff} .

The net suppression of star formation by turbulence has consequences in the diffuse, stratified interstellar medium of galaxies. This was demonstrated (34) with a well-resolved model of supernova driving of turbulence, including a treatment of radiative heating and cooling, but not self-gravity of the gas, run with the Flash adaptive mesh refinement gas dynamics simulation code (42). The turbulent flow indeed compressed gas into Jeans-unstable regions of cold, dense gas with sizes comparable to observed star-forming clouds. However, if the SFR expected for those regions is computed, it is an order of magnitude less than the rate required to produce the assumed number of supernovas driving the turbulence. This is consistent with the results of uniformly-driven, self-gravitating turbulence described in the preceding paragraph. Turbulence triggers star formation inefficiently; it does not lead to stochastic propagating waves of star formation as once envisioned by (43).

At the scale of single star-forming clouds, the question of triggering has also been studied (44). Here the most important effect is heating of the gas from under 100 K to around 10^4 K when UV radiation from newly formed massive stars ionizes it (45). The resulting huge increase in pressure drives a blast wave outwards. This strongly disturbs the morphology of the gas cloud. However, the actual difference in the SFR is small, accelerating the formation of stars by only 20% of the free-fall time of the cloud.

Quantitative observational studies support the conclusion that triggering does not represent a major mode of star formation. Although triggered star formation clearly occurs around regions of massive star formation, it is a relatively small effect that does not explain most star formation, consistent with the 10% effectiveness found by (34). For example, even under favorable circumstances, compression of gas by nearby massive stars triggers less than a quarter of star formation in the Elephant Trunk Nebula (46). At the galactic scale, multiple supernova explosions sweep up supershells in the Large Magellanic Cloud. Only 12–25% of the star-forming gas traced by the emission of the molecule carbon monoxide in the supershells formed as a direct result of supershell formation, corresponding to no more than 11% of the total star-forming gas in this galaxy (47).

What are the Sources of the Interstellar Turbulence?

If turbulence limits star formation, then understanding sources of turbulence, both in the diffuse gas and in dense clouds of star-forming, molecular gas, will help us to understand star formation.

Supernova explosions effectively drive turbulence in the diffuse gas (36). A study (48) of the velocity dispersion resulting from supernova rates ranging from the Milky Way value to 512 times higher, as would be seen in extreme starburst galaxies having SFRs hundreds of times that of the Milky Way, showed that, regardless of the supernova rate, supernova driving resulted in a rather uniform velocity dispersion $v_{\text{rms}} = 5\text{--}10 \text{ km s}^{-1}$. This work varied the surface density of the gas disks following the Kennicutt-Schmidt law (49) relating the surface density to the SFR, and thus the supernova rate. To simulate observations in the 21 cm line of atomic hydrogen, they fit single Gaussian components to the velocity of gas in the atomic temperature range (roughly

10^2 – 10^4 K). The resulting simulated observations showed spectral line widths equivalent to 10 – 20 km s $^{-1}$, agreeing with most observations (50, 51), aside from extreme starbursts where elevated 21 cm line widths are observed (52).

The driving of interstellar turbulence in nearby galaxies was more generally studied by (51) in a sample of galaxies observed with the Spitzer Infrared Nearby Galaxies Survey (53) and The H I Nearby Galaxies Survey (54). The energy input from supernovas can explain the observed density of kinetic energy of the interstellar gas within the star-forming inner regions of the observed disk galaxies. However, in the primarily gaseous outer disks, where star formation drops off strongly, so there are few supernova explosions, some other mechanism has to be stirring the gas to maintain the observed density of kinetic energy.

Two possibilities have been proposed for this alternative mechanism. One possibility is magnetorotational instability (55), which transfers energy from differential rotation into turbulence whenever the angular velocity decreases outward in rotating, magnetized gas. Galactic disks have flat rotation curves, with constant orbital velocity, because they lie within massive haloes of dark matter. Therefore their angular velocity indeed decreases outward, so magnetorotational instability can drive substantial turbulence (56).

The strength of this turbulence depends, however, on the thermal properties of the gas. The temperature dependence of the cooling curve for interstellar gas at $T < 10^4$ K leads to the possibility of a two-phase medium, in which the gas has two stable equilibria with the radiative heating (57), one cold ($T \sim 10^2$ K) and dense ($n \sim 100$ cm $^{-3}$) phase, and one warm ($T \sim 10^4$) and lower density ($n \sim 1$ cm $^{-3}$) phase. Simulations have shown that velocity dispersions of the magnitudes observed in 21 cm emission can be reached if such a two-phase medium forms (58). The energy input from the magnetorotational instability appears sufficient to explain the kinetic energy seen in the outer disks of galaxies beyond the star-forming region where supernovas are expected (51).

Another possibility, though, is that radiative heating from external sources of UV radiation such as quasars or starburst galaxies can by itself maintain the observed velocity dispersion as thermal motion (59, 60). Under this hypothesis, gas in the outer disk must lie predominantly in the warm phase, and the transition to a two-phase medium as density increases marks the radius at which star formation begins. This model can be distinguished observationally from magnetorotational instability by its prediction of an absence of gas in the cold, dense phase in outer disks. The discovery of finite rates of star formation in outer disks by the GALEX satellite UV observatory (61), however, suggests the presence of the cold, dense phase, supporting magnetorotational instability as the second driving mechanism.

Recently, radiation pressure from the light emitted by the most massive star clusters reflecting off of dust grains in the interstellar gas has been argued to play a major, or even dominant, role in limiting star formation in galaxies (52). However, this conclusion depends on how well radiation can couple to the dust, and thence with the gas by collisions of moving dust grains with the surrounding gas particles. If each photon from the massive stars only scatters once off of a dust grain before escaping the system, then the radiation pressure from a star cluster with luminosity L is proportional to L/c , where $c = 3 \times 10^5$ km s $^{-1}$ is the speed of light. This is

sometimes called the momentum-driven limit, as this conserves the momentum of the radiation, but much of its energy escapes. If, on the other hand, the dust is extremely optically thick, so that the photons continue scattering off of the dust until they lose almost all their energy, then the radiation pressure is far higher, proportional to L/v_{rms} , called the energy-driven limit. Because the turbulent motions in interstellar gas have $v_{\text{rms}} \sim 10 \text{ km s}^{-1}$, this represents a huge difference.

Although it is unlikely that the energy-driven limit is ever reached in real star-forming galaxies, the argument for the importance of radiation pressure relies on the expectation that the number of times the photons scatter is comparable to the infrared optical depth τ_{IR} of the most massive star-forming regions in the galaxies, which can be over 100. This assumption suggests a radiation pressure proportional to $\tau_{\text{IR}}L/c$. Several groups (62, 63) argued instead for the momentum-driven limit actually being the appropriate one, however, suggesting that radiation pressure is far less important in galactic evolution.

Recent multi-dimensional simulations of radiation pressure acting on a layer of gas with optical depth $\tau_{\text{IR}} \gg 1$ (64) showed that the radiation acts as a rarefied fluid accelerating a dense fluid, which causes Rayleigh-Taylor instability. The instability overturns and fragments the dense gas, indeed stirring it, but allowing the radiation to escape far more quickly than would be expected from its initial optical depth. As a result of this overturn, although radiation pressure indeed is more effective than the momentum-driven limit, it is typically at least an order of magnitude less efficient than suggested by the assumption of proportionality to $\tau_{\text{IR}}L/c$. This calls into serious question results based on that assumption.

The gravitational interaction of the gas with itself can temporarily drive turbulence even in the absence of outside energy inputs. Such gravitationally-driven turbulence indeed occurs in disks that are dense and cool enough to be subject to gravitational instability (25). The resulting turbulence produces a distribution of surface density fluctuations consistent with observations of atomic gas in the Magellanic Clouds. However, turbulence decays in roughly a gravitational free-fall time (65) so turbulence driven by internal gravitational motions cannot effectively delay gravitational collapse and subsequent star formation on its own.

On the other hand, accretion of gas from the intergalactic medium onto galaxies, a process that appears to continue to the present day, carries substantial kinetic energy with it, so it could feed gravitationally-driven turbulence. Even if that energy only couples to the interstellar gas with 10% efficiency, the velocity dispersion observed in the gas of galaxies comparable in mass to the Milky Way could be maintained if they accrete gas at the same rate as they form stars (66). Lower mass dwarf galaxies have lower accretion velocities, though, and so gain less energy. Nevertheless, they have the same observed velocity dispersion, which cannot be explained by this mechanism. Such dwarf galaxies represent the dominant location for star formation over cosmic time (67), so other mechanisms than accretion, such as supernova driving, must play an important role in its regulation.

Accretion may, however, indeed dominate the dynamics of individual star-forming clouds. They appear to continually accrete gas from the surrounding interstellar medium at a rate sufficient to drive the turbulent motions of $1\text{--}5 \text{ km s}^{-1}$ observed within them (66, 68, 69). This

results in longer lifetimes than would be expected for isolated clouds of the same mass, because the driven turbulence inhibits collapse and star formation. However, other forms of feedback such as ionization heating appear necessary to explain how star formation within these clouds comes to an end and the dense gas disperses.

Models of galactic evolution do lead us to one firm conclusion: driving of turbulence by internal gravity or accretion onto galaxies must be supplemented by other energy sources, as (66) argued must be true at least for dwarf galaxies. Otherwise, standard simulations performed without stellar feedback or other energy sources beyond gravity would be sufficient to reproduce observed galaxies, which is not the case, as summarized by (28), and simulated at high resolution in small, isolated dwarfs by (70). Insufficient numerical resolution leading to excessive dissipation of turbulent energy may play a role in massive galaxies, but not in the well-resolved dwarf simulations. Ultimately, gravity must compete with stellar feedback and other energy sources to determine the progression of collapse and star formation.

Star Formation Laws

Star formation correlates well with gas surface density in galaxies. The most well-known version of this correlation, the Kennicutt-Schmidt law (49), relates the SFR surface density Σ_{SFR} to the total (both atomic and molecular) gas surface density Σ_{gas} averaged over either the entire disks of normal or starburst galaxies, or entire galactic centers to derive the empirical law

$$\Sigma_{\text{SFR}} \propto \Sigma_{\text{gas}}^{1.4}. \quad (2)$$

Although variations around this law have been repeatedly found, for example in (71), it nevertheless appears to broadly hold (72). As observations reached higher resolution and were able to resolve regions a few thousand light years on a side in nearby galaxies, a similar correlation was found for them (73). However, in this case (Fig. 3a), regions with the lowest gas surface densities have lower SFR densities than would be expected from the power-law correlation, whereas the highest gas surface densities have higher than expected rates. Comparison to nearby star forming regions in the Milky Way shows that individual molecular clouds dozens of light years in size form stars far more efficiently than the larger regions observable in external galaxies (74). The rates observed in local clouds have been successfully simulated using high-resolution simulations of super-Alfvénic, isothermal turbulence (75).

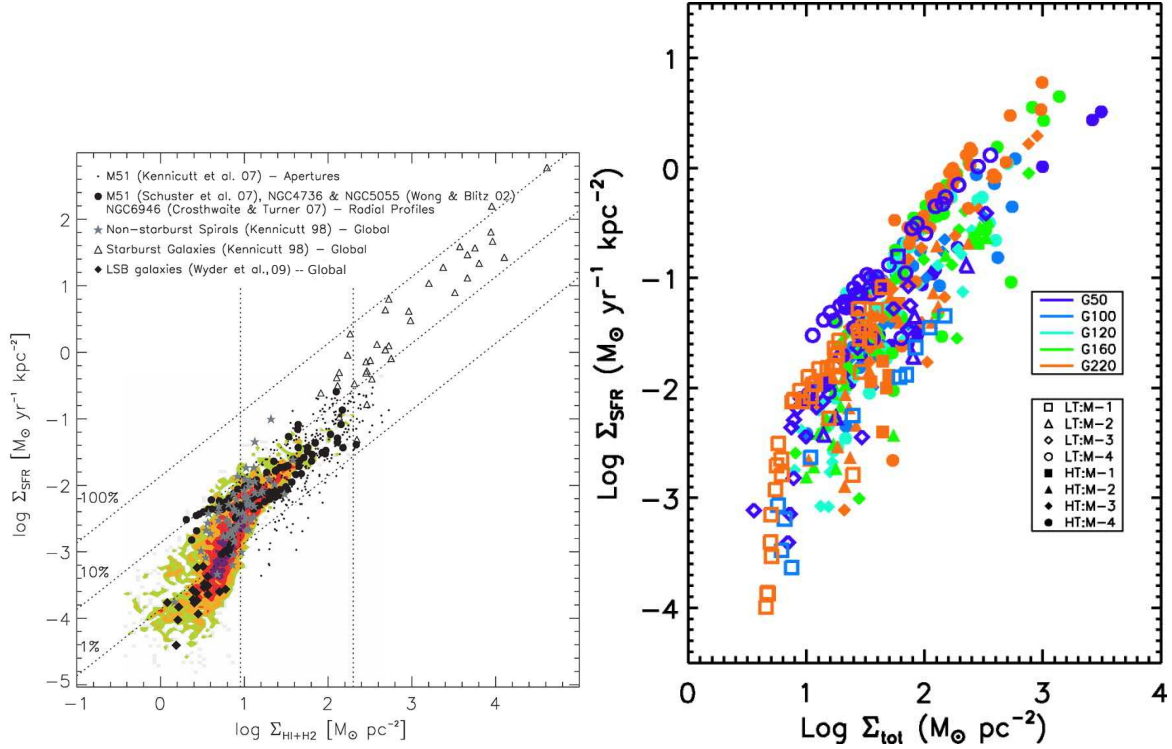


Figure 3: **Star formation correlations.** (a) A comparison of SFR surface density Σ_{SFR} to total gas surface density Σ_{gas} from observations presented in (73) showing the combined data from that paper in colored contours, along with points from the observations described in the legend on the figure (49, 77, 128–131). The dashed lines show what percentage of the gas would be consumed at that SFR over a period of 10^8 yr. (b) Radial profiles across model disks simulated with isothermal gas and live stellar disks and dark matter halos (132), showing the same drop in star formation efficiency at low gas surface density.

Star formation rate Observers derive SFRs from different observational indicators that trace either directly or indirectly the ionizing UV radiation from massive stars. Such stars have short lifetimes of only a few million years, so their presence traces recent star formation. The dense gas and dust immediately around newly forming stars absorbs UV light efficiently, ionizing and heating up in the process and reemitting the energy in the far infrared. Eventually the expanding bubble of ionized gas escapes the cloud. That gas can be observed in the $H\alpha$ line (the 2-1 transition of recombining atomic hydrogen), which lies in the red portion of the visible spectrum. After the young stars have entirely escaped their natal gas, they can be directly observed in the UV.

Determination of the total gas surface density depends on observation of not just the atomic hydrogen that dominates the diffuse interstellar gas, but also the H_2 that forms in the dense, star-forming clouds. However, the lowest rotational lines from the low-mass H_2 molecule lie at such high energies that they are not excited at the low temperatures typical of molecular gas (e.g. (72)). Instead, emission from the next most common molecule, carbon monoxide, is used as a tracer of the molecular gas. This requires the use of a conversion factor X_{CO} that has been found to be roughly constant in the Milky Way. However, it has recently been demonstrated (121–124) that the conversion factor rises sharply in regions with low absorption due to either low column density of gas and dust, or low heavy element abundance leading to low dust fractions in the gas. Conversely, it seems to drop in high column density regions dominated by molecular gas (125), such as in starburst galaxies (126).

While star formation deviates from the power law correlations with total gas in extreme cases, it correlates linearly with H_2 surface density over the entire range of observed values (73, 76–79), although with more than an order of magnitude scatter among individual regions. This has been interpreted to mean that H_2 formation causes or controls star formation (62, 80–82). However, one must ask whether correlation actually implies causation.

Indeed other measurements of high density gas ($n > 10^4 \text{ cm}^{-3}$) also show linear correlations of the column density of the gas with star formation. These include a linear correlation between HCN emission, which only occurs above a critical density $n_c \sim 10^5 \text{ cm}^{-3}$, and Σ_{SFR} (83); and a direct correlation between the number of young stellar objects in a region, and the mass of material with infrared extinction in the $2 \mu\text{m}$ K-band $A_K > 0.8$ (84) magnitude.

Examination of the physics of star formation reveals that molecule formation is not vital to the process of gravitational collapse, so long as heavy elements such as carbon and oxygen are present even in trace quantities $> 10^{-5}$ the solar abundance. It had been argued that low-energy molecular lines were required to allow radiative cooling of star-forming gas to only a few tens of degrees above absolute zero. Molecular gas does, in fact, dominate the cooling of such high density gas, but this is coincidental: pure atomic gas at the same densities cools almost as effectively by radiation from fine structure lines of heavy elements. Instead, the key factor for star formation seems to be shielding of the cold gas by dust from heating by background UV light (85, 86). Removing molecular cooling from models changes the minimum temperature from 5 K to 7 K, whereas removing the shielding increases the minimum temperature by more than an order of magnitude (86). Indeed, well-resolved galaxy formation simulations reached

virtually the same result whether star formation was limited to occur only in molecular gas, or allowed to occur in all dense gas (87).

The correlation observed between H_2 and star formation rate surface densities appears not to be causal, but rather to occur because both have a common cause. Formation of H_2 occurs over a timescale (88) of $t_f = (1 \text{ Gyr})/(n/1 \text{ cm}^{-3})$. As stars form through gravitational collapse, high densities are inevitably reached, and H_2 then forms quickly (89). This happens almost independent of the dust-to-gas ratio (90), which is largely controlled by the abundance of heavy elements, even though H_2 formation depends on dust surfaces. The dust grains provide the necessary catalyst for formation of a homonuclear molecule at densities low enough that three-body collisions hardly ever occur. (An exception to the need for dust surfaces occurs in the almost radiation-free environment of the early universe where electrons and protons can act as catalysts in gas phase reactions involving the fragile H^- and H_3^+ ions).

Collapse occurs within a free-fall time (91). However, at solar elemental abundances, cooling occurs far more quickly, with the cooling time $t_{\text{cool}} < t_{\text{ff}}$ for abundances as low as 10^{-4} of the solar abundance, characteristic of the early universe or the very lowest abundance dwarf galaxies in the local neighborhood. In such low abundance gas, molecule formation is delayed severely compared to the near solar abundance gas characteristic of the Milky Way. Then H_2 only forms in the very densest cores of the collapsing region, leading to low integrated molecular fractions, despite ongoing star formation.

Gravitational Instability

The gravitational instability of the gas and stars in galaxies does appear to control star formation directly. We can heuristically derive (36, 60) the criterion for stability of a differentially rotating galactic disk (92, 93) by comparing the free-fall time required for collapse of a region to the time required for it to shear apart, or for a pressure wave to cross it. We consider a thin galactic disk with uniform sound speed c_s and surface density Σ . The Jeans criterion for gravitational instability requires that the time scale for collapse of a density perturbation of size λ

$$t_{\text{ff}} = (\lambda/G\Sigma)^{1/2} \quad (3)$$

not exceed the time required for the gas to respond to the collapse by changing its pressure, the sound crossing time

$$t_s = \lambda/c_s. \quad (4)$$

This implies that regions can collapse if they have size

$$\lambda > c_s^2/G\Sigma. \quad (5)$$

In a rotating disk, collapsing perturbations effectively rotate around themselves because of Coriolis forces (92, 94), causing centrifugal motions that can also support against gravitational collapse if the collapse time scale t_{ff} exceeds the rotational period $t_{\text{rot}} = 2\pi\kappa$, where the epicyclic

frequency κ is of order the rotational frequency of the disk Ω . Thus, for collapse to proceed,

$$\lambda < 4\pi^2 G\Sigma/\kappa^2. \quad (6)$$

Gravitational instability occurs if there are regions with sizes that satisfy both of these criteria simultaneously, having

$$\frac{c_s^2}{G\Sigma} < \lambda < \frac{4\pi^2 G\Sigma}{\kappa^2}. \quad (7)$$

This occurs if the Toomre parameter (92)

$$Q \equiv c_s \kappa / (2\pi G\Sigma) < 1. \quad (8)$$

The full criterion for instability derived from linear analysis of the equations of motion of gas in shearing disks gives a factor of π rather than 2π in the denominator (93, 95), whereas using kinetic theory for collisionless stellar disks gives a factor of 3.36 (92).

When collisionless stars and collisional gas both contribute to gravitational instability, as in most galactic disks, a rather more complicated formalism is required to accurately capture their combined action (96, 97). This has been successfully approximated with simple algebraic combinations of the stellar and gas Toomre parameters (98, 99). Gas supported by turbulent flows rather than pure thermal pressure has no formal minimum wavelength for gravitational collapse in the presence of turbulent dissipation (94), although finite disk thickness does act to stabilize the smallest wavelengths against collapse.

Numerical simulations display the relationship between global gravitational instability and star formation. For example, (100) simulated the behavior of exponential gas disks embedded in live stellar disks, with the turbulent velocity in the disk modeled using an isothermal equation of state having a 6–12 km s⁻¹ sound speed. They varied the strength of the gravitational instability, and measured how much gas collapsed gravitationally in models that resolved the Jeans length to densities of $n \sim 10^7$ cm⁻³. They found not only that all of their models fell cleanly on the global Kennicutt-Schmidt correlation between total gas and SFR surface density, but also (Fig. 3b), that analysis of azimuthal rings in their models predicts the falloff in star formation at low gas densities observed at kiloparsec scales (73).

Another example of the strength of the hypothesis that gravitational instability controls star formation lies in the unusual morphologies of many high-redshift galaxies. Clumpy, irregular galaxies occur far more frequently at $z \sim 2$ than in modern times (101). Galaxies then tended to be far more gas-rich than now because gas accreted far more quickly in the denser high-redshift universe. As a result, high-redshift galaxies are more likely to be strongly gravitationally unstable. Well-resolved adaptive-mesh computations show that such conditions naturally lead to the formation of giant, gravitationally bound clumps (102) consistent with the observed morphologies.

An extended version of the gravitational instability hypothesis (103–106) proposes that star formation is controlled by the combination of gravitational instability and thermal equilibrium

in a two-phase medium. This occurs because stellar feedback increases as star formation increases, which in turn is driven by gravitational instability. However, as the feedback increases, it heats and stirs the gas. This reduces its gravitational instability as its effective pressure increases, and ultimately prevents gravitational instability entirely if the pressure increases beyond the range available to a two-phase medium. Thus, in this model, the star formation rate adjusts until a steady-state rate of star formation is reached.

Outlook

Understanding the cosmic history of star formation requires a statistical description of the luminosity function of galaxies, particularly of faint galaxies at early times. These faint galaxies dominate cosmic reionization (107) and can explain most of the apparent difference between star formation histories derived from gamma ray burst statistics and Lyman break galaxies (14). Heroic efforts with the final instrument set on the *Hubble Space Telescope* are yielding our first glimpses into this territory (107, 108), but real progress will occur with the next generation of ground and space based telescopes such as the *James Webb Space Telescope* (109), the European Extremely Large Telescope (110) and other 30 meter telescopes, and the Large Synoptic Survey Telescope (111).

Resolving feedback in simulations reaching cosmological scales remains tremendously difficult, but computers are slowly becoming sufficiently powerful and algorithms well developed enough for this to fall within the realm of the possible. Simulations of star formation over cosmic time that result in realistic star formation histories for single galaxies (87, 112) and even clusters of galaxies (113) have started appearing. Expanding these to statistically representative samples of the universe containing both clusters and voids remains a huge challenge that is just starting to be met (114). Use of adaptive spatial resolution on either structured (115, 116) or unstructured (114, 117) meshes² will clearly play a central role in making progress. Also required will be use of hybrid algorithms to take full advantage of massively parallel computer clusters made up of nodes with multiple processors sharing memory or even graphics coprocessors.

As our understanding of star formation comes into focus, we will be able to apply the knowledge gained to a series of outstanding questions. One is the evolution of heavy element abundances in galaxies, ultimately leading to planet formation around stars with sufficient rock-forming elements (118). Another is understanding the structure and origins of our own Milky Way galaxy, while a third is understanding how gas between galaxies both in clusters and in the field gets polluted with heavy elements and heated up to observed abundances and temperatures. Finally, the very structure of the cores of dark matter halos appears intertwined with star formation and feedback. Thus, improving our understanding of star formation will provide the key to unlocking the story of our own origins and those of the universe around us.

²see <http://www.cfa.harvard.edu/itc/research/movingmeshcosmology/> for visualizations of galaxies from unstructured mesh simulations

References

1. G. F. Smoot, *et al.*, *Astrophys. J. (Letters)* **396**, L1 (1992).
2. D. N. Spergel, *et al.*, *Astrophys. J. Suppl.* **170**, 377 (2007).
3. N. Jarosik, *et al.*, *Astrophys. J. Suppl.* **192**, 14 (2011).
4. Planck Collaboration, *et al.*, *Astron. Astrophys.* p. submitted (ArXiv: 1303.5062) (2013).
5. C. L. Bennett, *et al.*, *Astrophys. J. Suppl.* pp. submitted, (ArXiv: 1212.5225) (2012).
6. W. H. Press, P. Schechter, *Astrophys. J.* **187**, 425 (1974).
7. J. R. Bond, S. Cole, G. Efstathiou, N. Kaiser, *Astrophys. J.* **379**, 440 (1991).
8. S. D. M. White, C. S. Frenk, *Astrophys. J.* **379**, 52 (1991).
9. V. Springel, L. Hernquist, *Mon. Not. Roy. Astron. Soc.* **339**, 312 (2003).
10. P. Madau, *et al.*, *Mon. Not. Roy. Astron. Soc.* **283**, 1388 (1996).
11. S. J. Lilly, O. Le Fevre, F. Hammer, D. Crampton, *Astrophys. J. (Letters)* **460**, L1 (1996).
12. A. M. Hopkins, J. F. Beacom, *Astrophys. J.* **651**, 142 (2006).
13. V. Bromm, N. Yoshida, *Ann. Rev. Astron. Astrophys.* **49**, 373 (2011).
14. M. Trenti, R. Perna, E. M. Levesque, J. M. Shull, J. T. Stocke, *Astrophys. J. (Letters)* **749**, L38 (2012).
15. M. D. Kistler, H. Yüksel, J. F. Beacom, A. M. Hopkins, J. S. B. Wyithe, *Astrophys. J. (Letters)* **705**, L104 (2009).
16. B. E. Robertson, R. S. Ellis, *Astrophys. J.* **744**, 95 (2012).
17. C. C. Steidel, M. Giavalisco, M. Pettini, M. Dickinson, K. L. Adelberger, *Astrophys. J. (Letters)* **462**, L17 (1996).
18. R. J. Bouwens, *et al.*, *Astrophys. J.* **737**, 90 (2011).
19. B. P. Moster, T. Naab, S. D. M. White, *Mon. Not. Roy. Astron. Soc.* p. 321 (2012).
20. E. Costa, *et al.*, *Nature* **387**, 783 (1997).
21. R. Cen, J. P. Ostriker, *Astrophys. J.* **417**, 404 (1993).
22. N. Katz, D. H. Weinberg, L. Hernquist, *Astrophys. J. Suppl.* **105**, 19 (1996).

23. R. S. Somerville, J. R. Primack, *Mon. Not. Roy. Astron. Soc.* **310**, 1087 (1999).
24. D. Kereš, N. Katz, R. Davé, M. Fardal, D. H. Weinberg, *Mon. Not. Roy. Astron. Soc.* **396**, 2332 (2009).
25. F. Bournaud, B. G. Elmegreen, R. Teyssier, D. L. Block, I. Puerari, *Mon. Not. Roy. Astron. Soc.* **409**, 1088 (2010).
26. C. L. Dobbs, A. Burkert, J. E. Pringle, *Mon. Not. Roy. Astron. Soc.* **417**, 1318 (2011).
27. E. J. Tasker, *Astrophys. J.* **730**, 11 (2011).
28. C. B. Hummels, G. L. Bryan, *Astrophys. J.* **749**, 140 (2012).
29. A. Dalgarno, R. A. McCray, *Ann. Rev. Astron. Astrophys.* **10**, 375 (1972).
30. R. S. Sutherland, M. A. Dopita, *Astrophys. J. Suppl.* **88**, 253 (1993).
31. K. Tomisaka, S. Ikeuchi, *Publ. Astron. Soc. Japan* **38**, 697 (1986).
32. M.-M. Mac Low, R. McCray, M. L. Norman, *Astrophys. J.* **337**, 141 (1989).
33. M. A. de Avillez, *Mon. Not. Roy. Astron. Soc.* **315**, 479 (2000).
34. M. K. R. Joung, M.-M. Mac Low, *Astrophys. J.* **653**, 1266 (2006).
35. A. S. Hill, *et al.*, *Astrophys. J.* **750**, 104 (2012).
36. M.-M. Mac Low, R. S. Klessen, *Rev. Mod. Phys.* **76**, 125 (2004).
37. S. Chandrasekhar, *Roy. Soc. Lond. Proc. Ser. A* **210**, 26 (1951).
38. C. F. von Weizsäcker, *Astrophys. J.* **114**, 165 (1951).
39. R. S. Klessen, F. Heitsch, M.-M. Mac Low, *Astrophys. J.* **535**, 887 (2000).
40. C. Federrath, R. S. Klessen, *Astrophys. J.* **763**, 51 (2013).
41. P. Padoan, T. Haugbølle, Å. Nordlund, *Astrophys. J. (Letters)* **759**, L27 (2012).
42. B. Fryxell, *et al.*, *Astrophys. J. Suppl.* **131**, 273 (2000).
43. H. Gerola, P. E. Seiden, *Astrophys. J.* **223**, 129 (1978).
44. J. E. Dale, P. C. Clark, I. A. Bonnell, *Mon. Not. Roy. Astron. Soc.* **377**, 535 (2007).
45. B. G. Elmegreen, C. J. Lada, *Astrophys. J.* **214**, 725 (1977).
46. K. V. Getman, *et al.*, *Mon. Not. Roy. Astron. Soc.* **426**, 2917 (2012).

47. J. R. Dawson, *et al.*, *Astrophys. J.* **763**, 56 (2013).
48. M. R. Joung, M.-M. Mac Low, G. L. Bryan, *Astrophys. J.* **704**, 137 (2009).
49. R. C. Kennicutt, Jr., *Astrophys. J.* **498**, 541 (1998).
50. A. O. Petric, M. P. Rupen, *Astron. J.* **134**, 1952 (2007).
51. D. Tamburro, *et al.*, *Astron. J.* **137**, 4424 (2009).
52. N. Murray, E. Quataert, T. A. Thompson, *Astrophys. J.* **709**, 191 (2010).
53. R. C. Kennicutt, Jr., *et al.*, *Publ. Astron. Soc. Pacific* **115**, 928 (2003).
54. F. Walter, *et al.*, *Astron. J.* **136**, 2563 (2008).
55. S. A. Balbus, J. F. Hawley, *Rev. Mod. Phys.* **70**, 1 (1998).
56. J. A. Sellwood, S. A. Balbus, *Astrophys. J.* **511**, 660 (1999).
57. G. B. Field, *Astrophys. J.* **142**, 531 (1965).
58. R. A. Piontek, E. C. Ostriker, *Astrophys. J.* **663**, 183 (2007).
59. B. G. Elmegreen, A. Parravano, *Astrophys. J. (Letters)* **435**, L121 (1994).
60. J. Schaye, *Astrophys. J.* **609**, 667 (2004).
61. S. Boissier, *et al.*, *Astrophys. J. Suppl.* **173**, 524 (2007).
62. M. R. Krumholz, C. F. McKee, J. Tumlinson, *Astrophys. J.* **699**, 850 (2009).
63. S. M. Fall, M. R. Krumholz, C. D. Matzner, *Astrophys. J. (Letters)* **710**, L142 (2010).
64. M. R. Krumholz, T. A. Thompson, *Astrophys. J.* **760**, 155 (2012).
65. M.-M. Mac Low, *Astrophys. J.* **524**, 169 (1999).
66. R. S. Klessen, P. Hennebelle, *Astron. Astrophys.* **520**, A17 (2010).
67. A. Karim, *et al.*, *Astrophys. J.* **730**, 61 (2011).
68. E. Vázquez-Semadeni, P. Colín, G. C. Gómez, J. Ballesteros-Paredes, A. W. Watson, *Astrophys. J.* **715**, 1302 (2010).
69. N. J. Goldbaum, M. R. Krumholz, C. D. Matzner, C. F. McKee, *Astrophys. J.* **738**, 101 (2011).
70. C. M. Simpson, *et al.*, *Mon. Not. Roy. Astron. Soc.* pp. in press, (ArXiv:1211.1071) (2013).

71. R. Shetty, B. C. Kelly, F. Bigiel, *Mon. Not. Roy. Astron. Soc.* **430**, 288 (2013).
72. R. C. Kennicutt, N. J. Evans, *Ann. Rev. Astron. Astrophys.* **50**, 531 (2012).
73. F. Bigiel, *et al.*, *Astron. J.* **136**, 2846 (2008).
74. A. Heiderman, N. J. Evans, II, L. E. Allen, T. Huard, M. Heyer, *Astrophys. J.* **723**, 1019 (2010).
75. C. Federrath, R. S. Klessen, *Astrophys. J.* **761**, 156 (2012).
76. B. K. Rownd, J. S. Young, *Astron. J.* **118**, 670 (1999).
77. T. Wong, L. Blitz, *Astrophys. J.* **569**, 157 (2002).
78. A. K. Leroy, *et al.*, *Astron. J.* **136**, 2782 (2008).
79. F. Bigiel, *et al.*, *Astrophys. J. (Letters)* **730**, L13 (2011).
80. B. E. Robertson, A. V. Kravtsov, *Astrophys. J.* **680**, 1083 (2008).
81. N. Y. Gnedin, A. V. Kravtsov, *Astrophys. J.* **714**, 287 (2010).
82. C. Christensen, *et al.*, *Mon. Not. Roy. Astron. Soc.* **425**, 3058 (2012).
83. Y. Gao, P. M. Solomon, *Astrophys. J.* **606**, 271 (2004).
84. C. J. Lada, M. Lombardi, J. F. Alves, *Astrophys. J.* **724**, 687 (2010).
85. M. R. Krumholz, A. K. Leroy, C. F. McKee, *Astrophys. J.* **731**, 25 (2011).
86. S. C. O. Glover, P. C. Clark, *Mon. Not. Roy. Astron. Soc.* **421**, 9 (2012).
87. P. F. Hopkins, E. Quataert, N. Murray, *Mon. Not. Roy. Astron. Soc.* **417**, 950 (2011).
88. D. Hollenbach, E. E. Salpeter, *Astrophys. J.* **163**, 155 (1971).
89. S. C. O. Glover, M.-M. Mac Low, *Astrophys. J.* **659**, 1317 (2007).
90. S. C. O. Glover, P. C. Clark, *Mon. Not. Roy. Astron. Soc.* **426**, 377 (2012).
91. M. R. Krumholz, *Astrophys. J.* **759**, 9 (2012).
92. A. Toomre, *Astrophys. J.* **139**, 1217 (1964).
93. P. Goldreich, D. Lynden-Bell, *Mon. Not. Roy. Astron. Soc.* **130**, 97 (1965).
94. B. G. Elmegreen, *Astrophys. J.* **737**, 10 (2011).

95. V. S. Safronov, *Ann. Astroph.* **23**, 979 (1960).
96. C. F. Gammie, The formation of giant molecular clouds, Ph.D. thesis, Princeton Univ., NJ. (1992).
97. R. R. Rafikov, *Mon. Not. Roy. Astron. Soc.* **323**, 445 (2001).
98. B. Wang, J. Silk, *Astrophys. J.* **427**, 759 (1994).
99. A. B. Romeo, J. Wiegert, *Mon. Not. Roy. Astron. Soc.* **416**, 1191 (2011).
100. Y. Li, M.-M. Mac Low, R. S. Klessen, *Astrophys. J.* **639**, 879 (2006).
101. D. M. Elmegreen, *et al.*, *Astrophys. J.* **701**, 306 (2009).
102. O. Agertz, R. Teyssier, B. Moore, *Mon. Not. Roy. Astron. Soc.* **397**, L64 (2009).
103. E. C. Ostriker, C. F. McKee, A. K. Leroy, *Astrophys. J.* **721**, 975 (2010).
104. E. C. Ostriker, R. Shetty, *Astrophys. J.* **731**, 41 (2011).
105. C.-G. Kim, W.-T. Kim, E. C. Ostriker, *Astrophys. J.* **743**, 25 (2011).
106. R. Shetty, E. C. Ostriker, *Astrophys. J.* **754**, 2 (2012).
107. R. J. Bouwens, *et al.*, *Astrophys. J. (Letters)* **752**, L5 (2012).
108. M. Trenti, *et al.*, *Astrophys. J. (Letters)* **727**, L39 (2011).
109. J. P. Gardner, *et al.*, *Space Sci. Rev.* **123**, 485 (2006).
110. M. Lyubenova, M. Kissler-Patig, eds., *An expanded view of the Universe: Science with the European Extremely Large Telescope* (European Southern Observatory, 2009).
111. J. Tyson, *Proc. SPIE* **4836**, 10 (2002).
112. F. Governato, *et al.*, *Mon. Not. Roy. Astron. Soc.* **422**, 1231 (2012).
113. R. Cen, *Astrophys. J.* **741**, 99 (2011).
114. M. Vogelsberger, D. Sijacki, D. Kereš, V. Springel, L. Hernquist, *Mon. Not. Roy. Astron. Soc.* **425**, 3024 (2012).
115. A. V. Kravtsov, A. A. Klypin, A. M. Khokhlov, *Astrophys. J. Suppl.* **111**, 73 (1997).
116. B. W. O'Shea, *et al.*, *Adaptive Mesh Refinement: Theory and Applications*, e. a. T. Plewa, ed. (Springer, Heidelberg, 2004), pp. 341–350.

117. V. Springel, *Mon. Not. Roy. Astron. Soc.* **401**, 791 (2010).
118. L. A. Buchhave, *et al.*, *Nature* **486**, 375 (2012).
119. M.-M. Mac Low, *Molecular Gas, Dust, and Star Formation in Galaxies*, IAU Symposium 292, J. O. T. Wong, ed. (Cambridge U. Press, Cambridge, 2013), pp. 3–15.
120. J. H. Jeans, *Roy. Soc. Lond. Phil. Trans. Ser. A* **199**, 1 (1902).
121. S. C. O. Glover, M.-M. Mac Low, *Mon. Not. Roy. Astron. Soc.* **412**, 337 (2011).
122. D. Narayanan, M. Krumholz, E. C. Ostriker, L. Hernquist, *Mon. Not. Roy. Astron. Soc.* **418**, 664 (2011).
123. A. Schruba, *et al.*, *Astron. J.* **142**, 37 (2011).
124. R. Shetty, S. C. Glover, C. P. Dullemond, R. S. Klessen, *Mon. Not. Roy. Astron. Soc.* **412**, 1686 (2011).
125. D. Narayanan, M. R. Krumholz, E. C. Ostriker, L. Hernquist, *Mon. Not. Roy. Astron. Soc.* **421**, 3127 (2012).
126. D. Downes, P. M. Solomon, *Astrophys. J.* **507**, 615 (1998).
127. M. Trenti, *et al.*, *Astrophys. J. (Letters)* **714**, L202 (2010).
128. R. C. Kennicutt, Jr., *et al.*, *Astrophys. J.* **671**, 333 (2007).
129. K. F. Schuster, C. Kramer, M. Hitschfeld, S. Garcia-Burillo, B. Mookerjee, *Astron. Astrophys.* **461**, 143 (2007).
130. L. P. Crosthwaite, J. L. Turner, *Astron. J.* **134**, 1827 (2007).
131. T. K. Wyder, *et al.*, *Astrophys. J.* **696**, 1834 (2009).
132. Y. Li, M.-M. Mac Low, R. S. Klessen, *Astrophys. J.* **626**, 823 (2005).
133. An early version of this review was presented at IAU Symposium 292 (119). I have benefited over the past 15 years from discussions and collaborations on these topics with M. A. Avillez, B. G. Elmegreen, C. Federrath, S. C. O. Glover, F. Heitsch, A. S. Hill, M. R. Joung, R. S. Klessen, M. R. Krumholz, Yuexing Li, T. Peters, and E. Vázquez-Semadeni. I thank J. Beacom, C. Federrath, S. C. O. Glover, and J. C. Ibañez for useful comments on the manuscript, and the anonymous referees for detailed and constructive reviews that improved this work. I was partially supported by NSF grant AST11-09395, NASA Chandra Theory grant TMO-11008X, and DFG Sonderforschungsbereich 881—The Milky Way System.